NMR spectra of the product are identical with those obtained from methods A and B, except that the anion now also contains protons.

The corresponding aquo complex **1** can be fully analyzed, but the dihydrogen complex **2** loses $H_2$ in the solid state at 25 °C, so it cannot be analyzed.

**($\eta^2$-7,8-Benzoquinolinato)($\eta^2$-dihydrogen)hydridobis(tricyclohexylphosphine)iridium(III) Salts.** To $[IrH_5(PCy_3)_2]$ (410 mg, 0.54 mmol) in 15 mL of moist $CH_2Cl_2$ was added $PhCH(SO_2CF_3)_2$ (192 mg, 0.54 mmol) at -80 °C under $H_2$. After the solution stirred for 10 min, 7,8-benzoquinoline (97 mg, 0.54 mmol) was added, and at -80 °C $Et_2O$ was added to crystallize the dihydrogen complex **2** (L = $PCy_3$) as a white solid. $^1H$ NMR: (-80 °C $CD_2Cl_2$): -4.64 (br, Ir($H_2$)), -17.5 (br, Ir-H), 0.9-2.1 (c, $PCy_3$), 7.2-7.9 (Ar). $^1H$ NMR (20 °C, $CD_2Cl_2$): -10.34 (br, $IrH_3$). Carrying out the same synthetic procedure at 20 °C but with bubbling $N_2$ through the solution or pumping gently on it gives the corresponding aquo complex.

**Bis(dihydrogen)dihydridobis(tricyclohexylphosphine)iridium(III) Salts.** To $[IrH_5(PCy_3)_2]$ (20 mg, $2.64 \times 10^{-5}$ mol) in $CD_2Cl_2$ (0.5 mL) at -80 °C was added $PhCH(SO_2CF_3)_2$ (9.4 mg, $2.6 \times 10^{-5}$ mol). The resulting solution gave the following $^1H$ NMR spectrum. $^1H$ NMR ($CD_2Cl_2$, 188 K): -5.04 (v br, Ir($H_2$)), -15.26 (br, Ir-H), 0.9-2.1 (c, $PCy_3$). $^1H$ NMR ($CD_2Cl_2$, 25 °C): -8.33 (v br, $IrH_3$). The complex was characterized by $T_1$ measurements described in the text.

**Apparent $T_1$ Measurements.** These were obtained by inversion-recovery at -80 °C in $CD_2Cl_2$ at 500 MHz with a 180°-$t$-90° pulse sequence. We also looked at **2** (L = $PPh_3$) at 250 MHz.

**Isotherm Measurements.** These were determined on a vacuum line by comparing the pressure change in the vessel containing the complex, on admitting a fixed volume of $H_2$ to the sample, compared to admitting the same volume of He. The $H_2$ was passed through a Pd membrane to purify it. We thank Prof. Kurt Zilm for suggesting these measurements, which were carried out in the Chemical Engineering Department with the help of Dr. L. Bonneviot.

**Acknowledgment.** We thank the ARO (R.H.C.) and the NSF (M.L.) for support, Dr. G. J. Kubas, and Prof. R. H. Morris for preprints, Dr. E. Steifel and Profs. K. Zilm, J. H. Prestegard, and J. W. Faller for many helpful discussions, Dr. A. Siedle for a sample of $PhCH(SO_2CF_3)_2$, and P. Demou for experimental assistance. Douglas Hamilton in our group made some very helpful suggestions.

# Kinetics of Disproportionation of Tricarbonylbis(phosphine)iron(I) Cation Radicals Probed by Double Potential Step Chronocoulometry

**Michael J. Therien,[1a] Ching-Long Ni,[1b] Fred C. Anson,*[1b] Janet G. Osteryoung,[1c] and William C. Trogler*[1a]**

*Contribution from the Department of Chemistry, D-006, University of California, San Diego, La Jolla, California 92093, and the Division of Chemistry and Chemical Engineering, California Institute of Technology,[1d] Pasadena, California 91125.* *Received September 26, 1985*

**Abstract:** Rates of substitution of carbon monoxide in a series of iron(I) radical complexes were measured by using double potential step chronocoulometry, a transient electrochemical technique. Carbon monoxide substitution in $Fe(CO)_3L_2^+$ (L = a phosphine) radicals proceeds solely by a second-order process that is first order in both the metal radical and the entering pyridine nucleophile. The rate of substitution depends on the basicity and size of the Lewis base, as seen in the L = $PPh_3$ system, where $k_1$ varies over 400-fold from 0.27 to $1.01 \times 10^2$ $M^{-1}$ $s^{-1}$. Hammett analysis of the rate data shows that log $k_1$ correlates well with the $\sigma$-meta and $\sigma$-para values for nine 3- and 4-substituted pyridines. Nucleophilic attack of pyridine at $Fe(CO)_3(PCy_3)_2^+$ is $10^6$ times slower than at $Fe(CO)_3(PMe_3)_2^+$, presumably because increased phosphine ligand size inhibits the associative pathway. Activation parameters further support the proposed associative mechanism: for L = $PPh_3$, nucleophile = pyridine, $\Delta H^\ddagger = 9.8 \pm 0.3$ kcal $mol^{-1}$ and $\Delta S^\ddagger = -21 \pm 1$ cal $mol^{-1}$ $K^{-1}$; for L = $PCy_3$, nucleophile= 3,4-dimethylpyridine, $\Delta H^\ddagger = 14 \pm 1.5$ kcal $mol^{-1}$ and $\Delta S^\ddagger = -27 \pm 5$ cal $mol^{-1}$ $K^{-1}$. After substitution of carbon monoxide by a nitrogen Lewis base, these complexes disproportionate via an outer-sphere electron-transfer process to yield Fe(II) and Fe(0) products. Comparison of the reactivities of $Fe(CO)_3(PPh_3)_2$ and its 17-electron analogue, $Fe(CO)_3(PPh_3)_2^+$, shows that the cation radical is about $10^9$ more reactive toward pyridine than its 18-electron precursor.

Because of their role in catalytic and stoichiometric transformations,[2] there has been interest in reaction mechanisms of organometallic radicals. Studies of electrocatalysis of ligand substitution[3-6] and migratory insertion reactions,[7] of the lability of 17e species toward isomerization,[8] of radicals as oxidizing and reducing agents,[9] and of substitution labilities of stable organometallic radicals[10-13] illustrate the roles assumed by radicals in organotransition metal chemistry. Kinetic studies of simple organometallic radicals of the first transition series have been limited

(1) (a) University of California at San Diego. (b) California Institute of Technology. (c) Department of Chemistry, State University of New York, Buffalo, NY 14214. (d) Contribution No. 7297.

(2) (a) Brown, T. L. *Ann. N.Y. Acad. Sci. U.S.A.* **1980**, *333*, 80. (b) Kochi, J. K. *Organometallic Mechanisms and Catalysis*; Academic Press: New York, 1978. (c) Collman, J. P.; Hegedus, L. S. *Principles and Applications of Organotransition Metal Chemistry*; University Science Books: Mill Valley, CA, 1980. (d) Lappert, M. E.; Lendor, P. W. *Adv. Organomet. Chem.* **1976**, *14*, 345.

(3) Darchen, A.; Mahe, C.; Patin, H. *J. Chem. Soc., Chem. Commun.* **1982**, 243.

(4) Hershberger, J. W.; Kochi, J. K. *J. Chem. Soc., Chem. Commun.* **1982**, 212.

(5) Hershberger, J. W.; Klinger, R. J.; Kochi, J. K. *J. Am. Chem. Soc.* **1982**, *104*, 3034.

(6) Zizelman, P. M.; Amatore, C.; Kochi, J. K. *J. Am. Chem. Soc.* **1984**, *106*, 3771.

(7) (a) Magnuson, R. H.; Zulu, S.; T'sai, W.-M.; Giering, W. P. *J. Am. Chem. Soc.* **1980**, *102*, 6887. (b) Magnuson, R. H.; Meirowitz, R.; Zulu, S.; Giering, W. P. *Ibid.* **1982**, *104*, 5790.

(8) (a) Bond, A. M.; Grabaric, B. S.; Grabaric, Z. *Inorg. Chem.* **1978**, *17*, 1013. (b) Bond, A. M.; Grabaric, B. S.; Jackowski, J. J. *Ibid.* **1978**, *17*, 2153.

(9) Stiegman, A. E.; Goldman, A. S.; Leslie, D. B.; Tyler, D. R. *J. Chem. Soc., Chem. Commun.* **1984**, 632.

(10) Shi, Q.-Z.; Richmond, T. G.; Trogler, W. C.; Basolo, F. *J. Am. Chem. Soc.* **1982**, *104*, 71.

(11) Richmond, T. G.; Shi, Q.-Z.; Trogler, W. C.; Basolo, F. *J. Am. Chem. Soc.* **1982**, *104*, 76.

(12) McCullen, S. B.; Walker, H. W.; Brown, T. L. *J. Am. Chem. Soc.* **1982**, *104*, 4007.

(13) (a) Kidd, D. R.; Brown, T. L. *J. Am. Chem. Soc.* **1978**, *100*, 4095. (b) Beyers, B. H.; Brown, T. L. *Ibid.* **1977**, *99*, 2527. (c) Absi-Halabi, M.; Brown, T. L. *Ibid.* **1977**, *99*, 2982.

0002-7863/86/1508-4037$01.50/0 

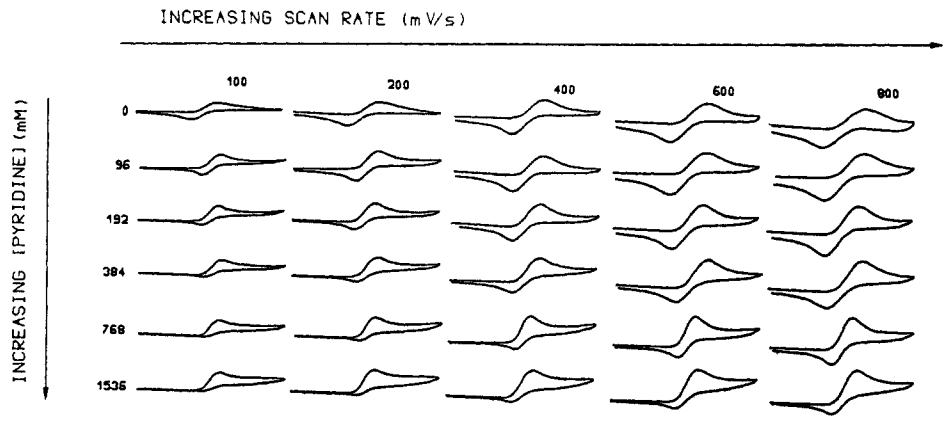


**Figure 1.** A matrix of cyclic voltammograms showing the dependence of the current ratio, $i_{pa}/i_{pc}$, on the concentration of the incoming nucleophile and the scan rate. Experimental conditions: $[Fe(CO)_3(PPh_3)_2] = 2 \times 10^{-3}$ M, [TBAP] = 0.1 M, temperature = −10.4 °C, $E_{1/2}[Fe(CO)_3(PPh_3)_2] = 0.064$ V (vs. a $Ag/AgNO_3$ (0.1 M) reference electrode), solvent = $CH_2Cl_2$, IR compensated over the potential range −0.5 (left) to +0.7 V (right).

to manganese,[6,8,12-14] chromium,[8,15] and vanadium[10,11] complexes. Only for vanadium has the size of the rate enhancement ($\sim 10^{10}$) in 17-electron complexes been quantified.[10,11] Since iron has the most extensively developed organometallic chemistry of any transition metal, it is important to define reactivities of 17e iron(I) species. Kochi's[16] investigation of metal formyl complexes derived from iron organometallic radicals and Krusic's[17] characterization of iron radical intermediates in the catalytic isomerization of olefins typify the recent interest about these species.

Syntheses and electrochemical generation of moderately stable $Fe(CO)_3L_2^+$ radicals (L = phosphine, phosphite, arsine) have been reported.[18a,19] These species provide an attractive system for elucidating reactivities of 17e iron(I) complexes. In a qualitative electrochemical study[19a] of these radicals it was claimed that nucleophiles such as acetonitrile "catalyze" a disproportionation reaction. Later quantitative EPR studies[19b] were taken as evidence for an unusual carbonyl bridged dinuclear dication in the reaction mechanism. The proposed iron(II) product species was not identified in either study, and the observation[19b] of phosphine oxides in the reaction solution raises questions about the mechanistic role of adventious oxygen. Spectroscopic evidence[18] shows that the iron cation radicals adopt a $D_{3h}$ trigonal bipyramidal geometry in contrast to the $C_{4v}$ structure assumed by the isoelectronic $Mn(CO)_5$ species. In this paper we describe kinetic and mechanistic studies of ligand substitution that leads to stoichiometric base-induced disproportionation of $[Fe(CO)_3(PR_3)_2]^+$ under anaerobic conditions. Double potential step chronocoulometry is shown to be a powerful technique for the rapid generation and mechanistic characterization of transient organometallic radicals.

## Results and Discussion

**Characterization of the Disproportionation Reaction.** Analytically pure $[Fe(CO)_3(PR_3)_2][PF_6]$ compounds (R = $C_6H_5$ = Ph or = c-$C_6H_{11}$ = Cy) can be isolated by using the method of Connelly,[18a] and complexes with smaller phosphines can be generated electrochemically in solution. Iron(I) cation radicals are most stable in $CH_2Cl_2$ solvent, with the tricyclohexyl derivative being the most resistant to disproportionation. Disproportionation, evidenced by appearance of neutral $Fe(CO)_3L_2$ in the IR spectrum, occurs at room temperature; however, addition of pyridine (eq 1) or other nucleophiles accelerates the process greatly. Spectrophotometric analysis of the reaction solution in the presence of 1,10-phenanthroline (eq 2) permitted quantification of the Fe(II) stoichiometry. Using the known IR extinction coefficient

$$2[Fe(CO)_3(PPh_3)_2]^+ + 6py \rightarrow Fe(CO)_3(PPh_3)_2 + [Fe(py)_6]^{2+} + 3CO + 2PPh_3 \quad (1)$$

$$[Fe(py)_6]^{2+} + 3phen \rightarrow [Fe(phen)_3]^{2+} + 6py \quad (2)$$

of $Fe(CO)_3(PPh_3)_2$, ($\epsilon_{max} = 4.9 \times 10^3$ $M^{-1}$ $cm^{-1}$) the characteristic absorbance at 1882.8 $cm^{-1}$ showed that 1 mol of $Fe(CO)_3(PPh_3)_2$ forms for every 2 mol of cation radical that reacts.

We propose a mechanism for disporportionation (Scheme I) similar to that we proposed[11] for $V(CO)_6$. Reaction 3 is probably irreversible since CO is an extremely poor nucleophile in comparison to pyridine ($k_1 \gg k_{-1}$). Reaction 4 leads to the formation of 16- and 18-electron organometallics derived from two 17-electron precursors. Formation of the stable 16- and 18-electron complexes provides a kinetic and thermodynamic sink so reaction 4 should be irreversible. Alternatively, a sequence of as many as three initial CO substitutions, the last being rate-determining, would yield equivalent kinetic behavior. This mechanism seems unlikely since no intermediate species (e.g., $Fe(CO)(py)_2L_2^+$) could be detected by FTIR spectroscopy for L = $PCy_3$ where the reaction took minutes to proceed at room temperature. Furthermore, examination of the reaction for L = $PPh_3$ by cyclic voltammetry (vide infra) did not show reduction waves for metastable pyridine-substituted iron(I) complexes.

**Scheme I**

$$Fe(CO)_3(PPh_3)_2^+ + py \underset{k_{-1}}{\overset{k_1}{\rightleftharpoons}} [Fe(CO)_2(py)(PPh_3)_2]^+ + CO \quad (3)$$

$$[Fe(CO)_2(py)(PPh_3)_2]^+ + [Fe(CO)_3(PPh_3)_2]^+ \xrightarrow{k_2} Fe(CO)_3(PPh_3)_2 + [Fe(CO)_2(py)(PPh_3)_2]^{2+} \quad (4)$$

$$[Fe(CO)_2(py)(PPh_3)_2]^{2+} + 5py \xrightarrow{fast} 2CO + 2PPh_3 + [Fe(py)_6]^{2+} \quad (5)$$

**Electrochemical Studies.** Transient electrochemical measurements can provide both thermodynamic and kinetic information.[6,15,16] Initial electrochemical studies of several $Fe(CO)_3L_2$ complexes by cyclic voltammetry revealed reversible to quasireversible behavior with formal potentials that span a wide range (−0.300–0.125 V) (Table I). Qualitative studies of the pyridine-induced disproportionation reaction were performed by adding known concentrations of pyridine to dry, degassed solutions of $Fe(CO)_3(PPh_3)_2$ in $CH_2Cl_2$. Addition of 60 mM pyridine to a 1 mM solution of $Fe(CO)_3(PPh_3)_2$ caused the reduction peak for $[Fe(CO)_3(PPh_3)_2]^+$ to disappear at scan rates as large as 800 mV $s^{-1}$. Cooling the electrochemical cell to −10.4 °C slowed the rate of disappearance of the Fe(I) complex sufficiently to allow cathodic peak currents to be observed as seen (Figure 1) in the matrix of cyclic voltammograms. The vertical columns of the matrix show

(14) McCullen, S. B.; Brown, T. L. *J. Am. Chem. Soc.* **1982**, *104*, 7496.
(15) Doxsee, K. M.; Grubbs, R. H.; Anson, F. C. *J. Am. Chem. Soc.* **1984**, *106*, 7819 and references therein.
(16) Narayanan, B. A.; Kochi, J. K. *J. Organomet. Chem.* **1984**, *272*, C49.
(17) Krusic, P. J.; Briere, R.; Rey, P. *Organometallics* **1985**, *4*, 801.
(18) (a) Baker, P. K.; Connelly, N. G.; Jones, B. M. R.; Maher, J. P.; Somers, K. R. *J. Chem. Soc., Dalton Trans.* **1980**, 579. (b) Therien, M. J.; Trogler, W. C. *J. Am. Chem. Soc.*, in press.
(19) (a) Blanch, S. W.; Bond, M. A.; Colton, R. *Inorg. Chem.* **1981**, *20*, 755. (b) Bagchi, R. N.; Bond, A. M.; Heggie, C. L.; Henderson, T. L.; Mocellin, E.; Seikel, R. A. *Ibid.* **1983**, *22*, 3007.

**Table I.** Cyclic Voltammetric Data[a] for $Fe(CO)_3L_2$ Complexes

| compound | $E_{1/2}$ (V)[b,c] | $i_{pa}/i_{pc}$[d] | $\Delta E_p$ (mV)[e] |
|---|---|---|---|
| $Fe(CO)_3(PPh_3)_2$ | 0.065 | 1.02 | 75 |
| $Fe(CO)_3(PCy_3)_2$ | −0.302 | 1.00 | 65 |
| $Fe(CO)_3(PMe_3)_2$ | −0.173 | 1.01 | 150 |
| $Fe(CO)_3[P(n\text{-}Bu)_3]_2$ | −0.088 | 1.00 | 160 |
| $FeCp_2$ | 0.125 | 1.00 | 60 |

[a] Experimental Conditions: $[Fe(CO)_3L_2] = 2 \times 10^{-3}$ M; supporting electrolyte = 0.1 M tetrabutylammonium perchlorate; temperature = 20 °C, scan rate = 200 mV/s; solvent = $CH_2Cl_2$; IR compensated. [b] Half-wave potentials relative to a Ag/0.1 M $AgNO_3$ reference electrode in acetonitrile. [c] Platinum disc working electrode. [d] Ratio of anodic to cathodic peak current. [e] Separation of anodic and cathodic peak positions.

that the lifetime of $[Fe(CO)_3(PPh_3)_2]^+$ decreases dramatically with increasing concentrations of pyridine, while the rows show the relationship between loss of the Fe(I) complex and duration of the voltammetric scan. Absence of a detectable response from the proposed $[Fe(CO)_2(py)(PPh_3)_2]^+$ species shows that reaction 4 is fast and irreversible as argued above. Voltammetric responses from the Fe(II) complexes generated in reactions 4 and 5 could not be sought at the more positive potentials where they would be expected because fouling of the electrode surface occurs.

Although the literature contains examples of quantitative analyses of the kinetics of pseudo-first-order reactions by cyclic voltammetry,[20] the approach is inherently limited by the requirement of Nernstian electrode kinetics or, lacking that, by the need to evaluate heterogeneous as well as homogeneous kinetic parameters from the data.[21] An additional drawback of this method is the difficulty in accurately measuring anodic to cathodic peak current ratios for voltammograms with poorly defined base lines. Techniques such as normal pulse and reverse pulse polarography[22] or double potential step chonocoulometry (DPSCC)[23] (where the electrode potential is maintained at a value corresponding to a reactant concentration of zero at the electrode surface throughout the kinetic measurement) are superior to cyclic voltammetry for the study of homogeneous reaction kinetics. In addition, working curves are available[24] from which kinetic parameters may be extracted for a variety of possible reaction mechanisms.

For these reasons the double potential step chronocoulometric method was employed to measure the rate of pyridine-induced disproportionation of Fe(I) cation radicals. The experiment consisted of stepping the potential from an initial value, $E_i$, where no electrode reaction was proceeding, to a final value, $E_f$, where the species of kinetic interest was generated at the electrode surface. The potential was held at $E_f$ for a time, $\tau$, after which it was stepped back to $E_i$ and maintained there for the same interval. During this period a portion of the reactant generated at $E_f$ is converted back to starting material. The charge that passes through the electrode during each of the time intervals is measured. The ratio of the two charges (after correction for background contributions as determined in blank experiments) provides a measure of the rate of any reaction that consumes the reactant generated at $E_f$. In the absence of a nucleophile the charge ratio $Q_R/Q_F$ was close to the expected value of 0.586[23] and independent of step duration ($\tau$) for all the substituted iron carbonyl bisphosphine derivatives examined. In the presence of a nucleophile the charge ratio decreases (Figure 2) with increasing concentration for a constant pulse width, $\tau$, and with increasing pulse width for a constant nucleophile concentration, consistent with the qualitative cyclic voltammetric observations.

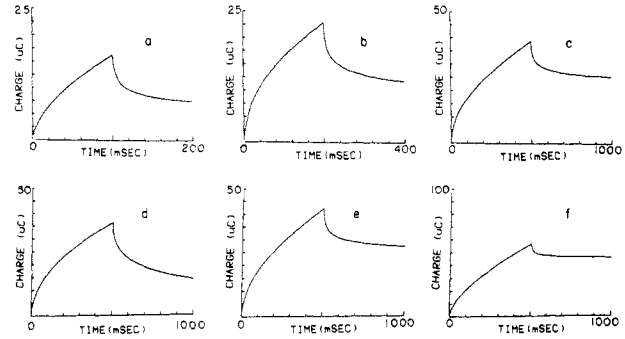


**Figure 2.** Double potential step chronocoulometry at varying pulse widths and nucleophile concentrations. Curves a through c are the $Q_F$ and $Q_R$ responses for a pyridine concentration of $60 \times 10^{-3}$ M and pulse widths of (a) 100 ms; (b) 200 ms; (c) 500 ms. Curves d through f are the responses for a pulse width, $\tau$, of 500 ms at pyridine concentrations of (d) 0; (e) $60 \times 10^{-3}$ M; (f) $180 \times 10^{-3}$ M. The response ratios, $Q_R/Q_F$, were calculated after correction of both $Q_R$ and $Q_F$ for background contributions as measured in blank experiments. Experimental conditions: $[Fe(CO)_3(PPh_3)_2] = 1 \times 10^{-3}$ M, [TBAP] = 0.2 M, temperature = 25 °C, solvent = $CH_2Cl_2$, $E = -300$ mV, $E_f = 750$ mV (vs. a Ag wire pseudo reference electrode).

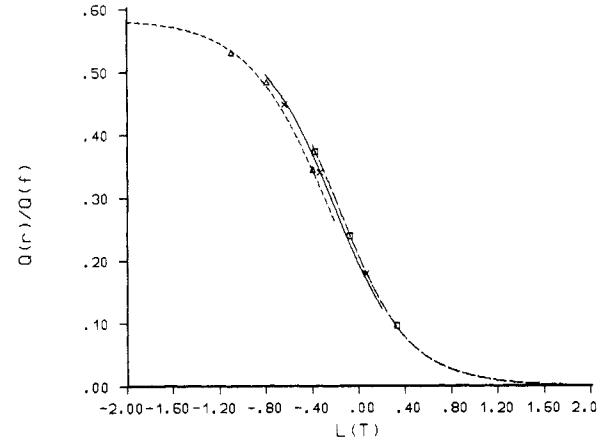


**Figure 3.** Variation of the charge ratio $Q_R/Q_F$ with the parameter $L(T) = \log (k_1[Nu]\tau)$ at different values of $k_2[A]/k_1[Nu]$. The relevant segments of the three working curves shown correspond to the following values of $k_2[A]/k_1[Nu]$: short dashed line = 25.0, solid line = 8.3, and long dashed line = 5.00. The triangles, crosses, and boxes correspond to the responses obtained from nucleophile concentrations of 60 mM, 180 mM, and 300 mM respectively. Experimental system: [A] = $Fe(CO)_3(PPh_3)_2$, [Nu] = pyridine, and $k_1$(evaluated) = 13.6 ± 0.6 $M^{-1}$ $s^{-1}$.

**Kinetics of Substitution and Disproportionation Reactions.** The mechanistic scheme exemplified by the reactions of Scheme I corresponds to the case labeled ECC in the terminology of ref 24, i.e., an electrode reaction (E) followed by two successive chemical reactions (CC). Expressed in its simplest terms, with both chemical reactions regarded as irreversible, the mechanism can be summarized as in Scheme II. Where $A = Fe(CO)_3(PPh_3)_2$, $A^+ = [Fe(CO)_3(PPh_3)_2]^+$, Nu is the added nucleophile, e.g., pyridine, $A(Nu)^+ = Fe(CO)_2(Nu)(PPh_3)_2^{2+}$, $A(Nu)^{2+} = Fe(CO)_2(Nu)(PPh_3)_2^{2+}$, and $A(Nu)_6^{2+} = Fe(Nu)_6^{2+}$. Reaction 7 is assumed to be irreversible because of the higher affinity of the

(20) (a) Nicholson, R. S.; Shain, I. *Anal. Chem.* **1964**, *36*, 706. (b) Nicholson, R. S. *Ibid.* **1966**, *38*, 1406. (c) Saveant, J. M. *Electrochim. Acta* **1967**, *12*, 999. (d) Saveant, J. M.; Vianello, E. *Electrochim. Acta* **1967**, *12*, 999. (e) Nicholson, R. S.; Shain, I. *Anal. Chem.* **1964**, *36*, 706. (f) Polcyn, D. S.; Shain, I. *Ibid.* **1966**, *38*, 376. (g) Mastragostino, M.; Nadjo, L.; Saveant, J. M. *Electrochim. Acta* **1968**, *13*, 721. (h) Mastragostino, M.; Saveant, J. M. *Ibid.* **1968**, *13*, 751. (i) Olmstead, M. L.; Nicholson, R. S.; *Anal. Chem.* **1969**, *41*, 862. (j) Nadjo, L.; Saveant, J. M. *Electrochim. Acta* **1971**, *16*, 87. (k) Feldberg, S. W. *J. Phys. Chem.* **1971**, *75*, 2377. (l) Feldberg, S. W.; Jeftic, L. *Ibid.* **1972**, *76*, 2349.

(21) (a) Feldberg, S. W. In *Electroanalytical Chemistry*; Bard, A. J., Ed.; Marcel Dekker: New York, 1969; Vol. 3, p 199. (b) Feldberg, S. W. *Computer Applications in Analytical Chemistry*; Mark, H. B., Ed.; Marcel Dekker: New York, 1972; Vol. 2, Chapter 7.

(22) (a) Korowa-Eisner, E.; Osteryoung, J. *Anal. Chem.* **1980**, *52*, 62. (b) Jackson, L. L.; Osteryoung, J.; Osteryoung, R. A. *Ibid.* **1980**, *52*, 67. (c) Osteryoung, J.; Hasabe, K. *Rev. Pol.* **1976**, *22*, 1.

(23) (a) Christie, J. H.; Anson, F. C.; Lauer, G.; Osteryoung, R. A. *Anal. Chem.* **1963**, *35*, 1979. (b) Bard, A. J.; Faulkner, L. R. *Electrochemical Methods*; Wiley: New York, 1980. (c) Christie, J. H.; Osteryoung, R. A.; Anson, F. C. *J. Electroanal. Chem.* **1967**, *13*, 236. (d) Christie, J. H. *Ibid.* **1967**, *13*, 79. (e) Anson, F. C. *Acc. Chem. Res.* **1975**, *18*, 400 and references therein.

(24) Hanafey, M. K.; Scott, R. L.; Ridgway, T. H.; Reilley, C. N. *Anal. Chem.* **1978**, *50*, 116.

**Table II.** Second-Order Rate Constants for Substitution of Carbon Monoxide by Pyridine in $Fe(CO)_3L_2^+$

| radical | $k_1$, $M^{-1}$ $s^{-1}$ | phosphine cone angle |
|---|---|---|
| $Fe(CO)_3(PMe_3)_2^+$ | 85[a] | 118 |
| $Fe(CO)_3(PPh_3)_2^+$ | 13.6 (±0.6)[a] | 145 |
| $Fe(CO)_3[P(n\text{-}Bu)_3]_2^+$ | 8.1[a] | 130 |
| $Fe(CO)_3(PCy_3)_2^+$ | $1.5 \pm 0.1 \times 10^{-4}$ [b] | 170 |

[a] Rate measured by using double potential step chronocoulometry and fitting the experimental responses to the theoretical working curve determined for the $Fe(CO)_3(PPh_3)_2$ system. Standard deviation in the measured rate constants for $Fe(CO)_3(PMe_3)_2$ and $Fe(CO)_3(P(n\text{-}Bu)_3)_2$ should be similar to that for $Fe(CO)_3(PPh_3)_2$ (±5% of the reported value). [b] Rate measured by monitoring the change in the visible absorption spectrum with time.

oxidized metal center for the added nucleophile (also present at much larger concentrations) than the carbon monoxide ligand that it displaces. In the presence of excess nucleophile the high rate of reaction 9 (cf. reaction 5) assures that reaction 8 is irreversible. Note that reaction 8 (cf. eq 4) is an outer-sphere electron-transfer reaction of the type described by Taube.[25]

**Scheme II**

$$A \underset{E_i}{\overset{E_f}{\rightleftharpoons}} A^+ + e \quad (6)$$

$$A^+ + Nu \xrightarrow{k_1} A(Nu)^+ + CO \quad (7)$$

$$A(Nu)^+ + A^+ \xrightarrow{k_2} A(Nu)^{2+} + A \quad (8)$$

$$A(Nu)^{2+} + 5Nu \xrightarrow{\text{fast}} A(Nu)_6^{2+} + 2CO + 2PR_3 \quad (9)$$

Working curves for the ECC mechanism that plot the expected values of the charge ratio, $Q_R/Q_F$, as a function of the dimensionless kinetic parameter, $k_1[Nu]\tau$, are available[24] for various values of $k_2[A]/k_1[Nu]$. Figure 3 contains segments of three such working curves along with the experimental values of $Q_R/Q_F$ for three different nucleophile (pyridine) concentrations. The appropriate working curves were selected by first finding the one that gave the best fit to the three data points for the lowest pyridine concentration. The second and third working curves were then determined by the values of $k_2[A]/k_1[Nu]$ corresponding to the higher concentrations of pyridine in the second and third set of experiments. As can be judged from Figure 3, the three sets of (three) data points can be accommodated well by the appropriate segments of the three working curves. The values of $k_1$ evaluated from the data points shown in Figure 3 are consistent and show no dependence on the pyridine concentration.

The average value of $k_1$, 13.6 ± 0.6 $M^{-1}$ $s^{-1}$ for the reaction between pyridine and $Fe(CO)_3(PPh_3)_2^+$, was combined with the parameter $(k_2[A]/k_1[Nu])$ characterizing the working curves that gave the best fit to the experimental points in Figure 3 to obtain an estimate of $k_2$ of $2 \times 10^4$ $M^{-1}$ $s^{-1}$. The working curves are insensitive to the value of $k_2$ when it becomes large so that this value of $k_2$ is best regarded as a lower limit.

The value of $k_2[A]/k_1[Nu]$ for the working curves in Figure 3 that gave the best fit of the data are large enough to allow an alternative reaction scheme to be ruled out. Reaction 8 of Scheme II could be replaced by a second electrode reaction in which $A(Nu)^+$ is oxidized to $A(Nu)^{2+}$ directly at the electrode instead of by an encounter with $A^+$ in the diffusion layer next to the electrode. Such ECE mechanisms have been the subject of considerable theoretical analysis and Saveant and Su[26] have shown recently that the ECE reaction pathway is negligible compared to the corresponding ECC pathway (e.g., Scheme II) whenever $k_2[A]/k_1[Nu] > 4$. We confirmed this prediction in the present case by comparing the temporal dependence of our values of $Q_F$ with those predicted for an ECE pathway.[27] The agreement was much poorer than that shown in Figure 3, which added to our confidence that the complexes examined in this study follow the mechanism depicted in Scheme II.

**Table III.** Observed Rate[a] Dependencies on Nucleophile[b] Concentration for $Fe(CO)_3(PPh_3)_2^+$ in $CH_2Cl_2$ at 25 °C

| $k_{obsd}$ | [nucleophile] (mM) |
|---|---|
| 0.81 | 60 |
| 2.34 | 180 |
| 4.26 | 300 |

[a] Measured by using double potential step chronocoulometry; rates reported are the average of the values obtained at three different pulse widths. [b] Pyridine. [c] $k_1 = 13.6 \pm 0.6$ $M^{-1}$ $s^{-1}$.

**Table IV.** Observed Rate[a] Dependencies on Nucleophile[b] Concentration for $Fe(CO)_3(PCy_3)_2^+$ in $CH_2Cl_2$ at 25 °C

| $k_{obsd} \times 10^{-4}$ $s^{-1}$ | [nucleophile] (mM) |
|---|---|
| 1.22 | 119 |
| 2.59 | 235 |
| 4.94 | 461 |
| 8.68 | 887 |

[a] Measured by spectrophotometric analysis. [b] 3,4-Dimethylpyridine. [c] $k_1 = 9.6 \pm 0.6 \times 10^{-4}$ $M^{-1}$ $s^{-1}$; intercept = $0.3 \pm .3 \times 10^{-4}$ $s^{-1}$.

**Table V.** Eyring Plot Data[a,b] for the Reaction between $Fe(CO)_3(PPh_3)_2^+$ and Pyridine

| $T^{-1} \times 10^{-4}$ | ln $(k_1/T)$ | $T^{-1} \times 10^{-4}$ | ln $(k_1/T)$ |
|---|---|---|---|
| 33.82 | −3.34 | 38.45 | −5.62 |
| 33.82 | −3.36 | 38.16 | −5.42 |
| 36.57 | −4.71 | 39.59 | −6.22 |
| 36.51 | −4.61 | 39.57 | −6.18 |

[a] Rates obtained by using double potential step chronocoulometry. [b] $\Delta H^\ddagger = 9.8 \pm 0.3$ kcal $mol^{-1}$; $\Delta S^\ddagger = -21 \pm 1$ cal $mol^{-1}$ $K^{-1}$.

Second-order rate constants, $k_1$, for pyridine substitution at $Fe(CO)_3L_2^+$ were also evaluated electrochemically for $Fe(CO)_3[P(n\text{-}Bu)_3]_2^+$ and $Fe(CO)_3(PMe_3)_2^+$. Reactions of $Fe(CO)_3(PCy_3)_2^+$ proceeded too slowly for the chronocoulometric technique to be practical. The kinetics of this substitution reaction were therefore followed by monitoring changes in the visible absorption spectrum ($\lambda$ = 655 nm) as a function of time. Rate data for various $Fe(CO)_3L_2^+$ radicals along with Tolman's cone angles[28] for the phosphine ligands are listed in Table II. The $10^6$ decrease in rate between the $PMe_3$ and $PCy_3$ derivatives must result from increased steric crowding in the 6-coordinate associative transition state. Plots of $k_{obsd}$ vs. nucleophile concentration for the reaction between $Fe(CO)_3(PPh_3)_2^+$ and pyridine and for the reaction between $Fe(CO)_3(PCy_3)_2^+$ and 3,4-dimethylpyridine (Tables III and IV) show a first-order dependence on incoming nucleophile. Since no nucleophile independent (i.e., dissociative) reaction pathway exists under the experimental conditions, the second order rate law is established.

$$-d[Fe(CO)_3L_2^+]/dt = k_1[Fe(CO)_3L_2^+][Nu]$$

This conclusion agrees with the ECC disproportionation mechanism (Scheme II) in which the initial ligand substitution determines the rate.

**Activation Parameters.** Rates of reaction of both $Fe(CO)_3(PPh_3)_2^+$ and $Fe(CO)_3(PCy_3)_2^+$ with nitrogen donor bases were determined at temperatures over a 45 °C range (25 to −20 °C). Derived activation parameters provide further support for an associative process. For the reaction between $Fe(CO)_3(PPh_3)_2^+$ and pyridine, $\Delta H^\ddagger$ and $\Delta S^\ddagger$ were determined to be 9.8 ± 0.3 kcal $mol^{-1}$ and −21 ± 1 cal $mol^{-1}$ $K^{-1}$, respectively. The reaction between $Fe(CO)_3(PCy_3)_2^+$ and 3,4-dimethylpyridine yielded a higher enthalpy of activation ($\Delta H^\ddagger$ = 14 ± 1.5 kcal $mol^{-1}$) and a lower activation entropy ($\Delta S^\ddagger$ = −27 ± 5 cal $mol^{-1}$ $K^{-1}$). Small enthalpies of activation and large negative entropies of activation

(25) Taube, H. *Electron Transfer Reactions of Complex Ions in Solution*; Academic Press: New York, 1970.
(26) Su, K. B.; Saveant, J. M. *J. Electroanal. Chem.*, in press.
(27) MacDonald, D. D. *Transient Techniques in Electrochemistry*; Plenum Press: New York, 1977.
(28) Tolman, C. A. *Chem. Rev.* **1977**, *77*, 313.

**Table VI.** Eyring Plot Data[a,b] for the Reaction between 3,4-Dimethylpyridine and $Fe(CO)_3(PCy_3)_2^+$

| $T^{-1} \times 10^{-4}$ | ln $(k_1/T)$ |
|---|---|
| 33.54 | −12.63 |
| 35.32 | −14.05 |
| 36.61 | −14.62 |
| 37.94 | −15.75 |

[a] Rates obtained by using visible absorption spectroscopy. [b] $\Delta H^{\ddagger}$ = 14.0 ± 1.5 kcal mol$^{-1}$; $\Delta S^{\ddagger}$ = −27 ± 5 kcal mol$^{-1}$ K$^{-1}$.

**Table VII.** Rate Constants[a] for Substitution of CO in $Fe(CO)_3(PPh_3)_2^+$ with Substituted Pyridines

| Nucleophile | $k_1$ (M$^{-1}$ s$^{-1}$) |
|---|---|
| 3,4-dimethylpyridine | 100 |
| 4-methylpyridine | 64 |
| 3-methylpyridine | 52 |
| pyridine | 13.6 ± 0.6[b] |
| 4-acetylpyridine | 4.9 |
| 3-fluoropyridine | 0.76 |
| 3-chloropyridine | 0.61 |
| 4-cyanopyridine | 0.33 |
| 3-cyanopyridine | 0.27 |
| 2,6-dimethylpyridine | 3.0 |
| 2,6-di-*tert*-butylpyridine | 0.54 |

[a] Experimental conditions: $[Fe(CO)_3(PPh_3)_2]$ = 1 × 10$^{-3}$ M, TBAP = 0.2 M, temperature = 25.0 °C, solvent = $CH_2Cl_2$; $E_i$ = −250 mV; $E_f$ = +750 mV (potentials relative to a silver wire pseudo reference electrode). [b] Since the mechanism of the reaction should be invariant to changes in the steric and electronic properties of the entering nitrogen Lewis base, the rate constants for all nucleophiles were obtained from the same working curves (Figure 3) generated for the appropriate values of $k_2[A]/k_1[Nu]$.

are typical[29,30] for reactions with a transition state of higher coordination number than the ground state. Data for the Eyring plots of the $Fe(CO)_3(PPh_3)_2^+$ and $Fe(CO)_3(PCy_3)_2^+$ systems are summarized in Tables V and VI, respectively.

**Steric and Electronic Effects on CO Substitution.** By using the $Fe(CO)_3(PPh_3)_2^+$ system and the electrochemical techniques discussed, the second-order rate constants $k_1$ were determined for a series of substituted pyridines (Table VII). Variation of the rate of substitution with the nature of the incoming nucleophile agrees with the proposed associative pathway. In Table VIII the $pK_a$'s, log $k_1$'s, and the Hammett $\sigma$-meta and $\sigma$-para values[31-33] for the 3- and 4-substituted pyridines are compared. The negative slope (or sign of $\rho$) in the Hammett plot of Figure 4 shows that the transition state in the rate-determining step must be favored by increased electron-donation to the frontier orbital of the nitrogen Lewis base, while the large value of $\rho$ (−3.25) implies substantial redistribution of charge in the transition state. Both observations support an associative pathway that results in coordination sphere expansion about a cationic metal center.

Steric effects were examined by measuring the rates of substitution with 2,6-dimethylpyridine and 2,6-di-*tert*-butylpyridine nucleophiles. As expected for an $S_N2$ process, the value of $k_1$ for sterically hindered nucleophiles decreases greatly in comparison to the $k_1$ for pyridine (Table VII).

One might expect that an extremely bulky base such as 2,6-di-*tert*-butylpyridine would not react. The finding that this nucleophile slowly substitutes CO in $Fe(CO)_3L_2^+$ may result from traces of nucleophilic impurities but also agrees with previous studies[10] that showed basicity is the dominant effect for substitution at 17-electron metal centers. This is explained by noting that even though an associative reaction occurring at a metal–radical center leads to coordination sphere expansion, the transition state may have a long metal–nucleophile distance. A filled orbital from the nitrogen Lewis base attacks a half-filled d orbital of $Fe(CO)_3L_2^+$ to yield a formal iron–nucleophile bond order of one-half in the transition state. This net metal–nucleophile bonding interaction allows for the facile associative pathway.

**Table VIII.** Data Used for Hammett Analysis of the Substitution Rate for 3- and 4-Substituted Pyridines[a]

| nucleophile | log $k_1$ | $pK_a$[c,d] | $\sigma_{m,p}$[d] |
|---|---|---|---|
| 3,4-dimethylpyridine | 2.0 | 6.48 | −0.21 |
| 4-methylpyridine | 1.8 | 6.03 | −0.14 |
| 3-methylpyridine | 1.7 | 5.67 | −0.08 |
| pyridine | 1.2 | 5.21 | 0.00 |
| 4-acetylpyridine | 0.69 | 3.51 | 0.28 |
| 3-fluoropyridine | −0.12 | 3.02 | 0.36[b] |
| 3-chloropyridine | −0.21 | 2.81 | 0.40 |
| 4-cyanopyridine | −0.48 | 1.86 | 0.55 |
| 3-cyanopyridine | −0.56 | 1.35 | 0.64 |

[a] Experimental conditions—same as Table VII. [b] Estimated from ref 32. [c] $pK_a$ of the pyridinium/pyridine couple in water from ref 32. [d] The use of these values in this nonaqueous system is justified by the fact that the trend in $pK_a$'s of substituted pyridines is known to be the same in aprotic solvents (ref 33). Gas phase and aqueous values are compared in ref 33b.

**Table IX.** Second-Order Rate Constants for Substitution at Metal Carbonyl Radicals and Their Phosphine-Substituted Derivatives of the First Transition Series

| complex | nucleophile | $k$, M$^{-1}$ s$^{-1}$ | ref |
|---|---|---|---|
| $V(CO)_6$ | $PMe_3$ | 132.0 | 10 |
| $V(CO)_6$ | py | 1.22 | 11 |
| $V(CO)_5[P(n\text{-}Bu)_3]$ | THF | 2.67 × 10$^{-6}$ | 11 |
| $Mn(CO)_5$ | $PR_3$ | >10$^3$ | 13a |
| $Mn(CO)_3[P(n\text{-}Bu)_3]_2$ | CO | 42 | 12 |
| $Mn(CO)_3[P(i\text{-}Bu)_3]_2$ | CO | 0.32 | 12 |
| $Fe(CO)_3(PPh_3)_2^+$ | py | 13.6 | this work |
| $Fe(CO)_3(PMe_3)_2^+$ | py | 85 | this work |

## Summary and Conclusion

The trigonal bipyramidal ($D_{3h}$) $Fe(CO)_3L_2^+$ complexes are exceptionally labile when compared to their 18-electron counterparts. Substitution of carbon monoxide in these 17-electron species takes place solely by an associative mechanism as seen from the following: (1) the fit of electrochemical data to the theoretical responses for the proposed mechanism; (2) the effect of increased nucleophile concentration on the rate of substitution; (3) the magnitudes of the activation enthalpy ($\Delta H^{\ddagger}$) and activation entropy ($\Delta S^{\ddagger}$); (4) the effects on the substitution rates of the Fe(I) cation radicals caused by varying steric and electronic properties of entering nucleophile. Apparently the 17-electron pentacoordinate iron center expands its coordination sphere to six, thereby forming a 19-electron intermediate or transition state. Formation of a 19-electron complex is aided by the existing hole in the $d^7$ e′ orbital of the trigonal bipyramidal complex, which permits facile nucleophilic attack in comparison to electronically saturated organometallic systems. Neutral, 18-electron $Fe(CO)_3(PPh_3)_2$ reacts with pyridine at 25 °C with a specific rate of about 10$^{-8}$ M$^{-1}$ s$^{-1}$ (measuring the disappearance of reactant by FTIR spectroscopy). The quantitative comparison of the rates of reaction of $Fe(CO)_3(PPh_3)_2^+$ and its 18-electron counterpart with pyridine allows us to estimate that *associative CO substitution at the iron cation radical proceeds at least 10$^9$ times faster than at neutral $Fe(CO)_3(PPh_3)_2$*. The value for the rate enhancement is similar to the 10$^{10}$ rate acceleration found[10] for 17-electron $V(CO)_6$. The transition state may occur at a long metal–nucleophile bond distance, where two-center, three-electron bonding[10] helps to stabilize the 19-electron transition state. After loss of CO to form 17-electron $Fe(CO)_2(py)(PR_3)_2^+$, the poor acceptor

(29) (a) Wawersik, H.; Basolo, F. *J. Am. Chem. Soc.* **1967**, *89*, 4626. (b) Schuster-Woldan, H. G.; Basolo, F. *Ibid.* **1966**, *88*, 1657. (c) Thorsteinson, E. M.; Basolo, F. *Ibid.* **1966**, *88*, 3929. (d) Dobson, G. R. *Acc. Chem. Res.* **1976**, *19*, 300. (e) Darensbourg, D. J. *Adv. Organomet. Chem.* **1982**, *21*, 131.
(30) (a) Basolo, F.; Pearson, R. G. *Mechanisms of Inorganic Reactions*, 2nd ed.; Wiley: New York, 1967; pp 234. (b) Espenson, J. H. *Chemical Kinetics and Reaction Mechanisms*, 1st ed.; McGraw-Hill: New York, 1981; pp 116.
(31) Fisher, A.; Galloway, W. J.; Vaughan, J. *J. Chem. Soc.* **1965**, 3591.
(32) (a) Henderson, W. A., Jr.; Streuli, C. A. *J. Am. Chem. Soc.* **1960**, *82*, 5791. (b) Gordon, A. J.; Ford, R. A. In *Chemist's Companion*; Wiley: New York, 1972; p 145.
(33) (a) Clauguis, G.; Deronzier, A.; Serve, D.; Vieil, E. *J. Electroanal. Chem.* **1975**, *60*, 205. (b) Taagepera, M.; Henderson, W. G.; Brownlee, R. T.; Beauchamp, J. L.; Taft, R. W. *J. Am. Chem. Soc.* **1972**, *94*, 1369.

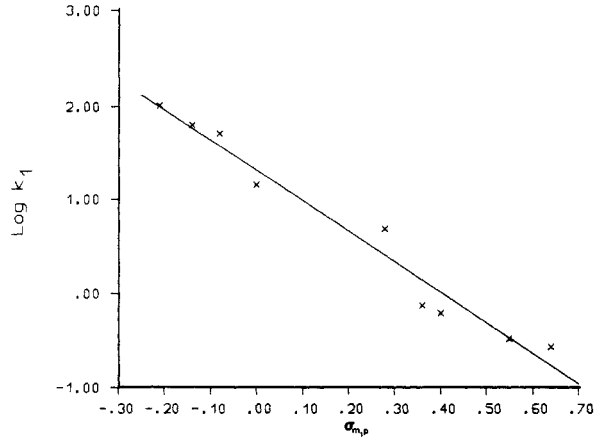


**Figure 4.** Hammett plot for the meta and para substituent effects on the rate of CO substitution at 25 °C (see Table VIII).

pyridine base increases the reducing power of the complex and results in fast outer-sphere electron transfer to $Fe(CO)_3(PR_3)_2^+$ and formation of Fe(II) complexes. This substitution–disproportionation reaction sequence has been previously observed[11] for $V(CO)_6$ and may prove to be a reaction pathway generally available to other 17-electron metal carbonyl radicals and their derivatives.

The kinetics reported herein have shown the utility and power of appropriate transient electrochemical techniques in the study of rapid chemical reactions that are coupled to electrode reactions. A comparison of rates of substitution at 17-electron iron with other first row, odd electron metal carbonyls and their phosphine substituted derivatives (Table IX) shows that rates of substitution decrease as the orbital containing the odd electron becomes sterically less accessible. Thus, in a particular metal system where CO ligands are replaced by phosphines or the steric bulk of the phosphines are increased, the rates decrease. Pentacoordinate metal radicals such as those studied here exhibit reactivities that greatly exceed hexacoordinate ones.

## Experimental Section

**Materials.** The $Fe(CO)_3L_2$ complexes were prepared photochemically from $Fe(CO)_5$ and the appropriate phosphine.[34] Iron pentacarbonyl (Strem), tri-*n*-butylphosphine (Aldrich), tricyclohexylphosphine (Strem), and triphenylphosphine (Strem) were used as received. Trimethylphosphine was synthesized from methyl magnesium iodide and triphenyl phosphite and redistilled twice before use. Various substituted pyridines (Aldrich) (3,4-dimethyl, 4-methyl, 3-methyl, 4-acetyl, 3-fluoro, 3-chloro, 2,6-dimethyl, and 2,6-di-*tert*-butyl) were stored over activated molecular sieves (Linde Type 4A) under an inert atmosphere for several days before use. Solid pyridine derivatives 3- and 4-cyanopyridine (Aldrich) were used without further purification. All materials were manipulated by standard Schlenk techniques. Manipulations of isolated iron(I) complexes were performed under $N_2$ in a Vacuum Atmospheres glove blox equipped with a HE-493 Dri-Train. Since the iron(I) compounds are slightly light sensitive, the electrochemical and kinetics experiments were carried out in the dark.

**Electrochemical Studies.** The supporting electrolyte (tetra-*n*-butylammonium perchlorate, Baker Polarographic Grade) was recrystallized twice from a mixture of ethyl acetate and isooctane (Burdick and Jackson) and dried in vacuo. Dichloromethane (analytical reagent, Mallinckrodt) was distilled from $CaH_2$ under nitrogen and stored under an inert atmosphere in a Schlenk flask. Pyridine (Aldrich Spectrophotometric Grade, Gold Label) was stored over KOH pellets for several days and then twice distilled from BaO under a nitrogen atmosphere. (Other pyridine derivatives were degassed and stored over activated molecular sieves.)

(34) Therien, M. J.; Trogler, W. C., submitted for publication in *Inorg. Synth.*

Cyclic voltammetry was performed with an IBM EC/225 voltammetric analyzer and displayed on an IBM 7424 x–y recorder. Double potential step chronocoulometric measurements were carried out with a BAS-100 Electrochemical Analyzer and BAS Model PL-10 digital plotter. The electrochemical cell was an IBM voltammetric cell assembly equipped with a thermostated jacket. The platinum disc-working electrode, the platinum wire auxiliary electrode, and the Ag/0.1 M $AgNO_3$ reference electrode (in $CH_3CN$) were also obtained from IBM Instruments.

Temperatures of solutions were measured by using a copper vs. constantan thermocouple with a reference junction of 0.0 °C. An Endocal constant temperature circulating bath was used to maintain the cell temperature. A blanket of nitrogen, which was presaturated with solvent at the same temperature, was maintained in the cell by continuous purging.

In a typical cyclic voltammetry experiment, 5 mL of a 0.1 M tetra-*n*-butylammonium perchlorate (TBAP) stock solution was syringed into the electrochemical cell, and the potential of the working electrode was cycled several times between the initial and final values. Then, 5 mL of a solution 4 mM in $Fe(CO)_3L_2^+$ complex and 0.1 M in TBAP was syringed into the cell along with a known concentration of nucleophile. Cyclic voltammograms were recorded at several scan rates, with stirring between each measurement. Working and auxiliary electrodes were cleaned with aqua regia after each set of experiments. In addition, the platinum disk-working electrode was polished occasionally with 0.3-$\mu$m alumina. Fouling of the platinum-working electrode surface occurred at potentials greater than 0.9 V vs. $Ag/Ag^+$ reference electrode, but reproducible voltammograms were obtained throughout the course of each set of experiments.

Chronocoulometric experiments were conducted with 0.2 M supporting electrolyte and 1.0 mM $Fe(CO)_3L_2^+$. A silver wire pseudo reference electrode was substituted for the $Ag/Ag^+$ reference electrode to avoid leakage of $Ag^+$ ions into the test solutions.

**Spectral Studies.** Infrared spectra were recorded by using an IBM FTIR/32. Visible absorption spectra were measured with an IBM 9420 UV–vis spectrophotometer equipped with a thermostated cell holder. Kinetic data for $[Fe(CO)_3(PCy_3)_2][PF_6]$ used 1 mM solutions of the complex and known nucleophile concentrations in 1.00-cm quartz cells equipped with a Teflon needle valve and ground glass joint. The reaction was followed by measuring the absorbance at 655 nm as a function of time. Plots of $\ln(A_\infty - A_t)$ vs. time were linear for more than 4 half-lives, and $k_{obsd}$ was determined from the slope of this line by least-squares analysis. All error limits represent a single standard deviation from unweighted least-square analysis. In the variable temperature studies, solvent and reactants were equilibrated to the appropriate temperature before mixing them in the cooled quartz cells.

**Synthesis of Tricarbonylbis(tricyclohexylphosphine)iron(I) Hexafluorophosphate.** This complex was prepared by a method similar[18a] to that used in the synthesis of $[Fe(CO)_3(PPh_3)_2][PF_6]$. After combining 0.84 g (2.9 mmol) of $AgPF_6$ and 1.45 g (3.0 mmol) of tri(4-bromophenyl)amine in 40 mL of $CH_2Cl_2$ and stirring for 5 min, the mixture was filtered through Kieselguhr (MCB) to remove metallic sliver. The dark blue solution was added to 2.0 g (2.9 mmol) of $Fe(CO)_3(PCy_3)_2$ dissolved in 40 mL of $CH_2Cl_2$ with continuous stirring to yield a green solution. After 5 min, hexane (50 mL) was added, the solution was filtered, and the solvent volume was reduced in vacuo to yield $[Fe(CO)_3(PCy_3)_2][PF_6]$ as an air-sensitive green solid, which was washed with toluene and dried in vacuo (yield: 1.55 g, 60%). Anal. Calcd for $C_{39}H_{66}F_6P_3O_3Fe$: C, 55.39; H, 7.87; P, 10.99. Found: C, 55.94; H, 7.73; P, 10.35.

**Acknowledgment.** We thank the National Science Foundation (Grant No's. CHE-84-02168 and CHE-85-04088 to W.C.T. and CHE-83-11579 to F.C.A.) for financial support. We thank Professor J. K. Kochi for a preprint of ref 6.

**Registry No.** $Fe(CO)_3(PMe_3)_2^+$, 102133-38-0; $Fe(CO)_3(PPh_3)_2^+$, 60243-26-7; $Fe(CO)_3[P(n\text{-}Bu)_3]_2^+$, 102133-39-1; $Fe(CO)_3(PCy_3)_2^+$, 102133-40-4; $[Fe(CO)_3(PCy_3)_2][PF_6]$, 102133-41-5; CO, 630-08-0; 3,4-dimethylpyridine, 583-58-4; 4-methylpyridine, 108-89-4; 3-methylpyridine, 108-99-6; pyridine, 110-86-1; 4-acetylpyridine, 1122-54-9; 3-fluoropyridine, 372-47-4; 3-chloropyridine, 626-60-8; 4-cyanopyridine, 100-48-1; 3-cyanopyridine, 100-54-9; 2,6-dimethylpyridine, 108-48-5; 2,6-di-*tert*-butylpyridine, 585-48-8.